Nanophotonics 1 (2012): 117–123 © 2012 by Walter de Gruyter • Berlin • Boston. DOI 10.1515/nanoph-2012-0007

Optical tuning and ultrafast dynamics of high-temperature superconducting terahertz metamaterials

Ranjan Singh[1,*], Jie Xiong[1,2], Abul K. Azad[1], Hao Yang[1,3], Stuart A. Trugman[1], Q. X. Jia[1], Antoinette J. Taylor[1] and Hou-Tong Chen[1,*]

[1] Center for Integrated Nanotechnologies, Los Alamos National Laboratory, Los Alamos, New Mexico 87545, USA, e-mail: ranjan@lanl.gov; chenht@lanl.gov

[2] State Key Lab of Electronic Thin Films and Integrated Devices, University of Electronic Science and Technology of China, Chengdu 610054, China

[3] Jiangsu Key Laboratory of Thin Films, School of Physical Science and Technology, Soochow University, Suzhou 215006, China

* Corresponding author

Abstract

Through the integration of semiconductors or complex oxides into metal resonators, tunable metamaterials have been achieved by a change of environment using an external stimulus. Metals provide high conductivity to realize a strong resonant response in metamaterials; however, they contribute very little to the tunability. The complex conductivity in high-temperature superconducting films is highly sensitive to external perturbations, which provides new opportunities in achieving tunable metamaterials resulting directly from the resonant elements. Additionally, superconducting metamaterials are expected to enable strong nonlinear response and quantum effects, particularly when Josephson junctions are integrated into the metamaterial resonant elements. Here we demonstrate ultrafast dynamical tuning of resonance in the terahertz (THz) frequency range in $YBa_2Cu_3O_{7-\delta}$ (YBCO) split-ring resonator (SRR) arrays excited by near infrared femtosecond laser pulses. The photoexcitation breaks the superconducting Cooper pairs to create quasiparticles. This dramatically modifies the imaginary part of the complex conductivity and consequently the metamaterial resonance on an ultrafast timescale, although the real conductivity does not change significantly. We observed resonance switching accompanied by substantial frequency tuning as a function of photoexcitation fluence, which also strongly depends on the nanoscale thickness of the superconducting films. All of our experimental results agree with calculations using an analytical model, which takes into account the contributions of the complex conductivity of the YBCO films to SRR resistance and kinetic inductance. The theoretical calculations reveal that the increasing SRR resistance upon increasing photoexcitation fluence is responsible for the reduction of resonance strength, and changes in both the resistance and kinetic inductance cause the resonance frequency shifts.

Keywords: Metamaterials; terahertz; high-temperature superconductor; split-ring resonator; photoexcitation; ultrafast dynamics.

1. Introduction

An important issue in resonant electromagnetic metamaterials is how to overcome the loss, particularly in the optical frequency range where the Drude response provides limited conductivity in metals [1–3]. However, one may also take advantage of the typically undesirable loss to realize functionalities such as switching and modulation of electromagnetic waves [4], where the metamaterial resonant response plays a critical role in obtaining strong enhancement of light-matter interactions. Based on such considerations, there have been many approaches developed to realize tunability in hybrid metamaterials, where materials including semiconductors and complex oxides serve as the metamaterial substrate or spacer, or are integrated into specific regions of metamaterial resonators [5–25]. The resonant response in hybrid metamaterials can be switched and/or frequency shifted when an external stimulus, such as temperature [5–8], voltage bias [9–14], or photoexcitation [15–25], is applied. The optical approach has received the most intensive attention in metamaterial photonics due to its simplicity, addressability, and capability of ultrafast tuning. However, in all of these approaches, the metals that compose metamaterial resonators contribute very little to the active components, merely providing high conductivity to realize a strong resonance.

It has been shown that metal conductivity as well as thickness can affect the metamaterial resonance [26, 27], although the tunability is through design and fabrication. Noble metals are still the material of choice for fabricating metamaterial structures because of their high conductivity, which, however, makes the resonance tuning rely on the integration of additional materials able to respond to external stimuli. The complex conductivity in high-temperature superconducting films is highly sensitive to external perturbations, including temperature, magnetic fields, optical excitation, and electrical current. In fact, there have been a few recent demonstrations of superconducting metamaterials, which are of particular interest in loss reduction and resonance tuning [28–38], the latter has mostly been achieved by a change of temperature [28–34, 37, 38] and application of magnetic fields [30, 35], two approaches that are uniquely suitable for manipulation of properties in superconductors. Although loss reduction in superconducting metamaterials is limited to frequencies up to the terahertz (THz) regime due to the strong frequency dependence of the complex conductivity as well as the energy band gap in superconductors, superconducting metamaterials

are expected to have great potential for THz generation [39] and detection [40], particularly when Josephson junctions are integrated into the structures.

In this work, we systematically investigate the resonant response, its tuning and dynamics under ultrafast near infrared photoexcitation in planar high-temperature superconducting THz metamaterials. The near infrared photons break the superconducting Cooper pairs to create quasiparticles, which dramatically modifies the imaginary part of the complex conductivity and consequently shifts the metamaterial resonance frequency. We observed the resonance switching accompanied with significant frequency tuning as a function of photoexcitation fluence, which also strongly depends on the nanoscale thickness of the superconducting films. We investigated experimentally the dynamics of the metamaterial resonance for various pump fluences, and the results are compared to and reproduced by calculations using an analytical model [29, 34], which takes into account the contributions of the complex conductivity of the superconducting films to both the SRR resistance and kinetic inductance. This work represents an important step towards nonlinear and quantum THz metamaterials to yield functionalities that are difficult or impossible to achieve through conventional approaches in this technically challenging frequency range, as the superconducting films can naturally exhibit strong nonlinear response and additional quantum devices – Josephson junction – can be integrated into the structures.

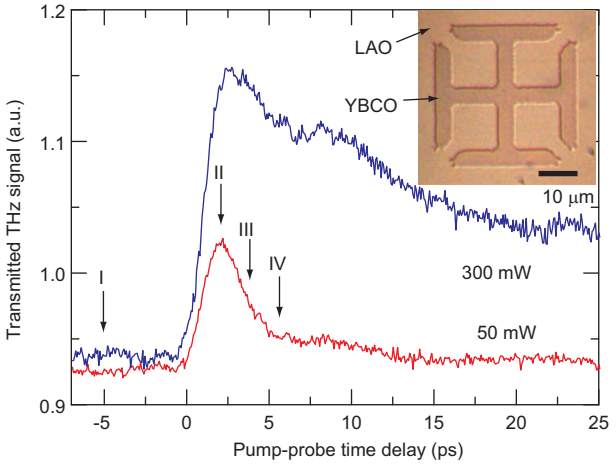

Figure 1 Dynamics of the 100-nm-thick YBCO metamaterial upon femtosecond near infrared photoexcitation. The transmitted THz peak signal was measured as a function of pump-probe time delay at 20 K for 50 and 300 mW photoexcitation powers. Position I indicates that the THz probe pulse has lower transmission due to the strong resonant response of the metamaterial sample when it arrives about 5 ps earlier than the optical pulse. At positions II, III and IV the THz pulse arrives after the optical excitation with different pump-probe time delays. Inset: a microscopic image of one unit cell of the 100-nm-thick YBCO metamaterial. For all measurements the normally incident THz radiation has the electric field polarized along one of the SRR arms (either in *x* or *y* direction).

2. Experiments and Results

Epitaxial $YBa_2Cu_3O_{7-\delta}$ (YBCO) high-temperature superconducting films with δ=0.05 and thicknesses of 50, 100, and 200 nm were prepared using pulsed laser deposition on (100) $LaAlO_3$ (LAO) substrates with dimensions of 10 mm×10 mm×0.5 mm, over which the thickness variation is <3%. The transition temperature was determined to be T_c=90 K by the ac susceptibility measurement, with a transition width of ~0.5 K. Square arrays of electric split-ring resonators (SRRs) [41], with a unit cell microscopic image shown in the inset to Figure 1, were fabricated from the YBCO films through conventional photolithographic methods and wet chemical etching using 0.01% H_3PO_4 solution for several minutes. However, we would like to point out that other types of SRR could also be used, i.e., the results in this work do not depend on the choice of geometry of SRRs. Under normal incidence, the YBCO films and metamaterials were characterized at a temperature of 20 K using an optical-pump THz-probe (OPTP) spectrometer [16, 42] incorporated with a continuous flow liquid helium cryostat. The output near infrared laser beam (50 fs, 3.2 mJ/pulse at 800 nm with a 1-kHz repetition rate) was split into two parts with one being used for THz generation-detection and the other for optical excitation (pump) of the YBCO films or metamaterial samples. The pump beam has a beam diameter of ~1 cm, much larger than the focused THz spot diameter of ~3 mm at the sample, providing mostly uniform excitation over the YBCO films and metamaterials. This, however, makes it difficult to precisely measure the sample temperature, due to laser heating under high fluence photoexcitation, because the temperature sensor has to be located at the copper sample holder rather than directly touching the top of sample to avoid the direct exposure to the pump laser. Variation of pump-probe time delay was realized using a motion stage to change the pump beam optical path. For various pump powers and pump-probe time delays, THz pulses transmitting through the YBCO films and metamaterials, as well as a blank LAO substrate as the reference, were measured in the time-domain, i.e., recording the time-varying electric field of the impulsive THz radiation. The transmission amplitude and phase spectra were directly obtained by performing fast Fourier transformation of the time-domain signal and normalized to that of the reference. The complex conductivity of the YBCO films was extracted from the measured transmission amplitude and phase spectra through the inversion of Fresnel equations [43].

Figure 1 shows the transmitted THz peak signal through a 100-nm-thick YBCO metamaterial at 20 K as a function of time delay between the near infrared pump and THz probe pulses, for two example optical pump fluences of 0.05 and 0.3 mJ/cm^2, or powers of 50 and 300 mW, respectively. At low temperatures, the highly superconducting YBCO film results in strong resonant response in the metamaterial structure, which causes a lower transmission of THz radiation. The near infrared photons break the superfluid Cooper pairs in the superconducting YBCO films and create the quasiparticles

which dramatically reduce the conductivity and metamaterial resonance, and therefore increase the transmitted THz signal starting from the pump-probe time zero shown in Figure 1. The ~2 ps rise time is mainly due to time duration of the THz pulses, which limits the time resolution. When the pump-probe time delay increases, the transmitted THz signal decreases due to the recombination of quasiparticles to form Cooper pairs. Under low fluence excitation, the relaxation time is approximately 5 ps, and there is a clearly observable second peak ~7 ps after the main transmission peak arising from reflected laser pulses at the back surface of the substrate. Increasing the pump fluence causes a larger relaxation time and results in a much longer tail, most likely due to thermal effects. We have also carried out similar measurements for bare YBCO films, and the results are very similar to those shown in Figure 1.

The amplitude spectra of THz transmission through the 100-nm-thick metamaterial sample were then measured at 20 K for various photoexcitation fluences at four time delays indicated by the arrows in Figure 1. In the absence of a pump pulse, the metamaterial exhibits a strong resonant response, as shown by the red curves in Figures 2A–2D with a resonant transmission minimum of 10% or power transmission of 1%, which is comparable to that in metamaterial samples fabricated from gold with the same thickness. This also facilitates the use of high-temperature superconductors in metamaterials replacing noble metals with additional tuning capability. Figure 2A shows the resonant transmission spectra for various pump powers when THz pulses pass through the metamaterial sample a few picoseconds before the optical pump pulses (time position I in Figure 1). The small resulting change indicates that the excitation in the YBCO metamaterial has relaxed nearly completely during the time interval of 1 ms between the optical pump pulses. Immediately following the femtosecond photoexcitation (time position II), the metamaterial resonance is significantly weakened and red-shifted with increasing pump power, as shown in Figure 2B. The resonance disappears at a pump power of 100 mW. Increasing the pump-probe time delay results in recovery of metamaterial resonance strength due to carrier relaxation, as revealed in Figures 2C and 2D for positions III and IV, respectively, both of which are before the arrival of the reflected optical pulse from the back surface of the substrate. With the same pump power, the resonance strength increases and its frequency shifts back when the time delay increases. However, when the pump power is high, e.g., 500 mW, the thermal effects last much longer and the metamaterial resonance does not recover within the time delay of tens picoseconds in our measurements, which is consistent with the dynamics measurements shown in Figure 1.

It has been shown that the resonance tuning in superconducting metamaterials through change of temperature is strongly dependent on the film thickness [34]. We also fabricated identical metamaterial structure from YBCO films with two other thicknesses of 50 and 200 nm. Measured at the pump-probe time delay position III, the pump power dependent resonant transmission spectra are shown in Figures 2E and 2F. These spectra reveal that increasing

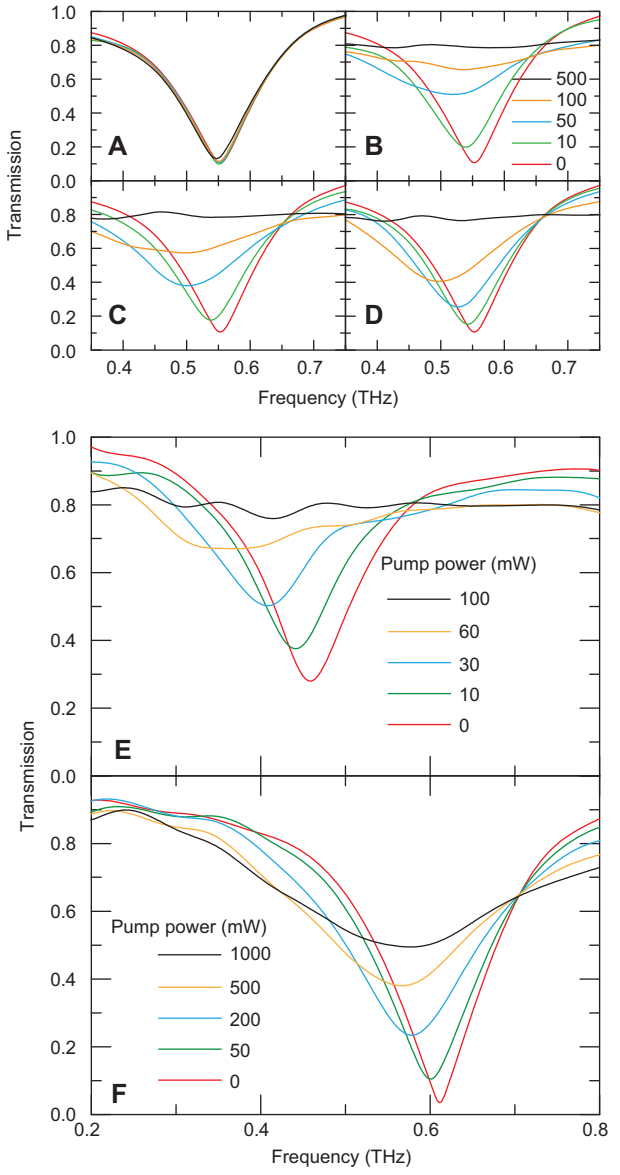

Figure 2 THz transmission amplitude spectra of YBCO metamaterials for various pump powers. The spectra shown in A–D are for the 100-nm-thick YBCO metamaterial at the respective pump-probe time positions I–IV. E and F, THz transmission amplitude spectra for YBCO metamaterials with 50 and 200 nm thicknesses, respectively, measured at the pump-probe time position III.

YBCO film thickness results in a higher resonance frequency, stronger resonance strength, smaller frequency tuning range, and requiring higher pump power in tuning the resonance. In the absence of a pump pulse, the resonance frequency is 0.460, 0.553, and 0.612 THz, and the resonance transmission minimum is 0.28, 0.11, and 0.03, respectively, for the YBCO metamaterials with thickness of 50, 100, and 200 nm. For the 50-nm-thick YBCO metamaterial, 100 mW pump laser power is sufficient to completely switch off the resonance; while for the 200-nm-thick YBCO metamaterial, even 1000 mW pump laser power is insufficient to switch off the resonance.

3. Discussion

The complex conductivity plays an essential role in the resonance tuning in high-temperature superconducting metamaterials [34]. Figure 3 shows the complex conductivity at 0.55 THz of the 100-nm-thick YBCO film, measured at 20 K as a function of pump power at four different pump-probe time delays shown in Figure 1. When there is no optical pump, the imaginary part is about one order of magnitude higher than the real part. For time position I, there is little change in the conductivity, shown in Figure 3A, with increasing pump power, which confirms that the 1 ms time interval of the laser pulses is sufficient for nearly-complete thermal relaxation. Shown in Figure 3B for the pump-probe time position II, the imaginary conductivity dramatically decreases by orders of magnitude as the superfluid Cooper pairs are broken into quasiparticles by the near infrared photons, while the real conductivity does not exhibit a significant change (at most a factor of 2) as it arises from the Drude response of quasiparticles. Shown in Figures 3C and 3D for the pump-probe time positions III and IV, respectively, the imaginary conductivity increases with increasing pump-probe time delay, which allows for recovery of the superfluid.

There have been a few discussions that surface resistance and kinetic inductance contribute to resonance tuning in superconducting metamaterials [29, 34]. The surface impedance (in Ω/Square) of a superconducting film can be calculated from the measured complex conductivity [34]:

$$\tilde{Z}_S = R_S - iX_S = Z_0 \frac{n_3 + i\tilde{n}_2 \cot(\tilde{\beta}d)}{\tilde{n}_2^2 - n_3^2} \cong i\frac{Z_0}{\tilde{n}_2}\cot(\tilde{\beta}d) \qquad (1)$$

where the "~" indicates a complex value, Z_0=377 Ω is the vacuum impedance, n_3=4.8 is the LAO substrate refractive index, $\tilde{n}_2 = \sqrt{i\tilde{\sigma}/\varepsilon_0\omega}$ is the complex refractive index of the YBCO film, $\tilde{\sigma}$ is the measured complex conductivity, $\tilde{\beta} = \tilde{n}_2\omega/c_0$ is the complex propagation constant where c_0 is the light velocity in vacuum, and d is the thickness of the superconducting film. The surface resistance R_S and reactance $X_S = \omega L_S$ are shown in Figure 4 as a function of pump power for the 100-nm-thick YBCO film, which are calculated at 0.55 THz and at different pump-probe time delays. The surface resistance R_S, which represents the loss, increases rapidly with pump power; while the surface reactance X_S increases first with lower pump power, reaches a maximum value, and then drops with further increasing pump power. As we compare the results in Figures 3 and 4, it is interesting to find that the maximum surface reactance, and therefore the maximal frequency tuning, occurs at a pump power where the real and imaginary parts of the complex conductivity are equal. However, this is not really surprising since it can be easily verified using Eq. (1).

At resonance, the SRR reactance is absent and the surface resistance of the SRR layer can be calculated from the YBCO surface resistance, $R = [(A-g)/w]R_S$, where A=64 μm is the circumference of the SRR current loop, g=4 μm is the split gap width, and w=4 μm is the strip width of the SRR. By treating the SRR layer as a shunt resistor in a transmission line, the resonant transmission minimum can then be calculated for the pump-probe time positions I–IV, with the results shown in Figures 5A–5D, respectively. Compared to the experimental results, which are also shown in Figure 5, there is good agreement, i.e., both the experiments and calculations reveal an increase in resonant transmission minimum (decreasing resonance strength) with pump power.

The frequency of the fundamental resonance in SRRs is typically given by $\omega_0 = 1/\sqrt{LC}$, where L and C are the loop inductance and gap capacitance, respectively. However, when the ohmic loss is significant, the resistance R in an equivalent circuit of SRR has to be considered [34]:

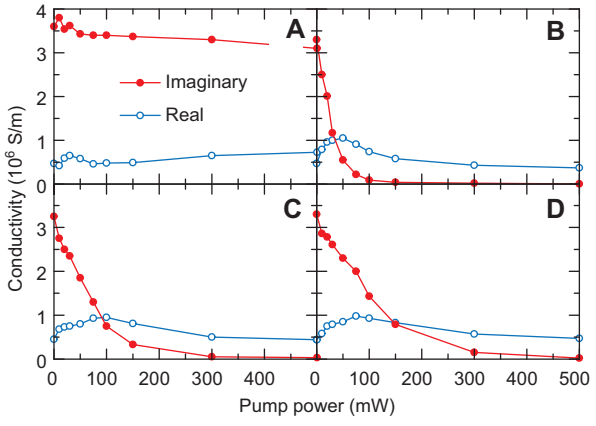

Figure 3 Experimentally measured complex conductivity at 20 K as a function of pump power for the 100-nm-thick bare YBCO film. A–D, Real and imaginary parts of the complex conductivity are retrieved at 0.55 THz for pump-probe time positions I–IV, respectively.

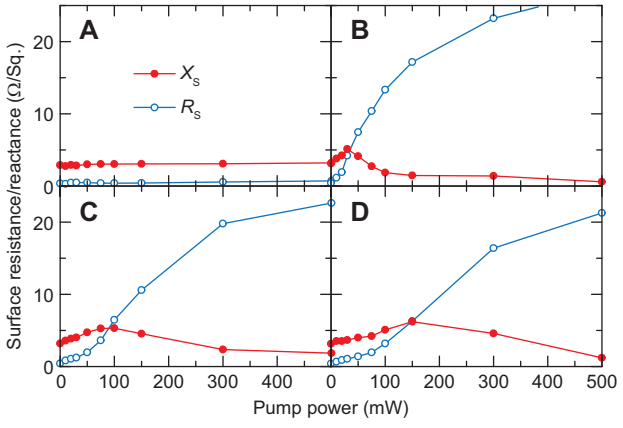

Figure 4 Calculated surface impedance as a function of pump power for the 100-nm-thick bare YBCO film. A–D, The surface resistance and reactance are calculated using the experimental conductivity shown in Figure 3 for the respective pump-probe time positions I–IV.

$$\omega_0^2=\frac{1}{LC}-\frac{R^2}{4L^2}. \quad (2)$$

In superconducting SRRs, the inductance L includes two contributions: Faraday inductance L_F which is determined and can be estimated by the geometry and dimensions of the SRR [44], and kinetic inductance $L_k=[(A-g)/w](X_S/\omega)$ which is associated with the kinetic energy in superconducting charge carriers. The capacitance C can be derived using Eq. (2) from simulated resonance frequency ω_0' when assuming perfect conducting SRR, i.e., $L=L_F$, $R=0$, and therefore $C=(\omega_0'^2 L_F)^{-1}$. With all these derived parameters, we can calculate the resonance frequency of the YBCO metamaterial as a function of pump power, as shown in Figures 5E–5H for the pump-probe time positions I–IV, respectively. It is again compared to the experimental results with good agreement. Here we have limited our discussion to 80 mW pump power due to the diminishing metamaterial resonance strength for further increasing pump power over 100 mW. Upon photoexcitation, both the resistance and inductance increase, and the overall effect is a reduction of resonance frequency. With increasing the pump-probe time delay both the resonance strength and frequency recover due to the reformation of Cooper pairs on an ultrafast timescale.

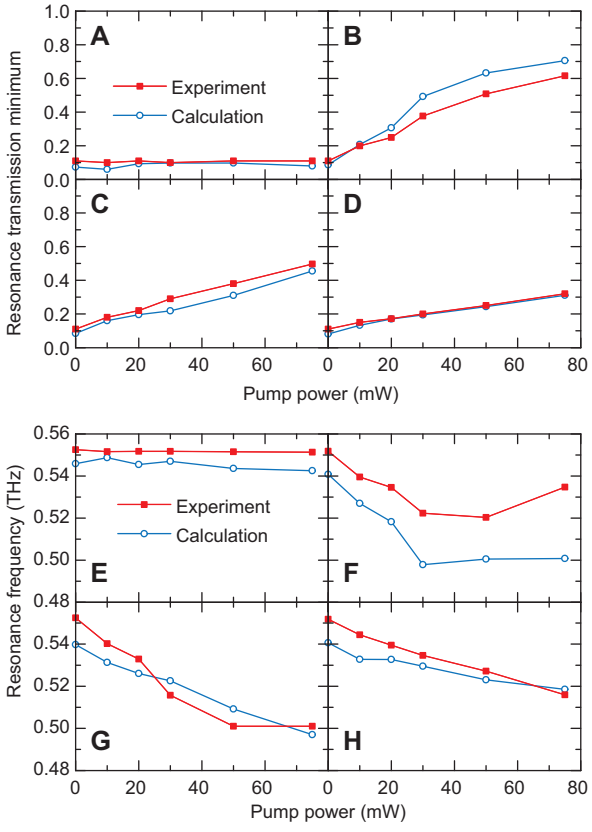

Figure 5 Experimentally measured and theoretically calculated transmission minimum and resonance frequency. A–D, Resonant transmission minimum, and E–H, resonance frequency as a function of pump power for the 100-nm-thick YBCO metamaterial sample at the pump-probe time positions I–IV, respectively.

Certainly, the complex conductivity in YBCO films is frequency dependent, in contrast to the assumption of frequency-independent conductivity taken at the resonance frequency in the above model calculations. However, this assumption does not affect the validity of this model because the change of conductivity is not significant in the relatively small frequency range around the resonance. Finally, the above model can also explain the thickness dependent YBCO metamaterial resonance and tuning shown in Figure 6. Although the thickness may affect the conductivity of the superconducting films, in all of our measurements the variation is <50%, even with the measurement error taken into account. For simplicity, we can assume thickness independent conductivity. According to Eq. (1), reducing the film thickness d results in a larger surface resistance R_S and consequently smaller resonance strength, i.e., a larger resonant transmission minimum, as verified in Figure 6A. Reducing the film thickness d increases the surface reactance X_S as well, and consequently results in a higher kinetic inductance L_K, although it also negligibly increases the Faraday inductance L_F [44]. For thin YBCO metamaterials, the kinetic inductance L_K could be comparable or even larger than the Faraday inductance L_F. Additionally, the change of L_K can be as large as $L_{K,20K}/2$ upon photoexcitation. As such, the overall effect is a lower resonance frequency, which could be predominantly caused by the increasing kinetic inductance, and a wider tuning range of the resonance frequency, as shown in Figure 6B, for reduced YBCO metamaterial thickness. The different pump power requirements for tuning of the resonant frequency in YBCO metamaterials of varying thicknesses may result from the limited penetration depth of the pump laser.

4. Conclusions

We have shown the ultrafast resonance tuning behavior in high-temperature superconducting THz metamaterials through femtosecond near infrared photoexcitation. Increasing the pump power results in a reduced resonance strength and red-shifting of frequency. Under low fluence photoexcitation, the relaxation time is ~5 ps; further increasing the pump fluence also introduces significant thermal effects with a much longer relaxation time. The dynamics of the metamaterial resonance follows that of the superconducting films. Using experimentally measured complex conductivity of the superconducting films, we are able to reproduce such behavior through calculations by including the ohmic resistance and kinetic inductance. The theoretical calculations reveal that the increasing SRR resistance upon increasing photoexcitation fluence is responsible for the reduction of the resonance strength, and both the resistance and kinetic inductance contribute to the shifting of the resonance frequency. We have also shown that the nanoscale thickness of the superconducting films plays an important role in the frequency tuning range and requirement of optical pump fluence. Thinner superconducting metamaterials require lower pump fluences to switch the resonance and result in a larger frequency tuning range.

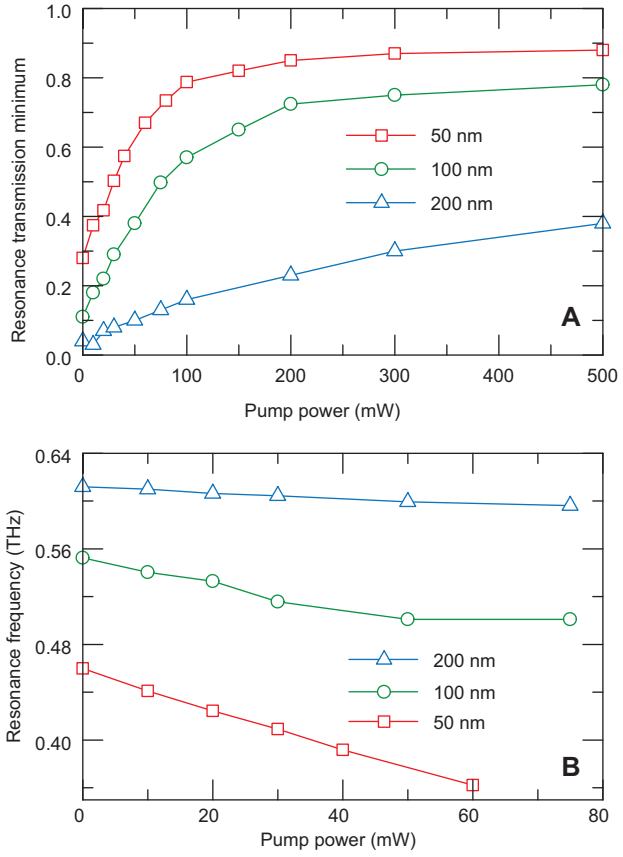

Figure 6 Experimentally measured resonance tuning for YBCO metamaterials of different thickness. A, Resonant transmission minimum, and B, resonance frequency as a function of pump power for the YBCO metamaterials of 50, 100, 200 nm thicknesses, measured at the pump-probe time position III.

While the demonstrated metamaterial resonance tuning is not practical at optical frequencies due to the superconducting energy gap, such ultrafast dynamical resonance tuning would be useful in realizing multifunctional microwave and THz metamaterial and plasmonic devices by further design and materials integration.

Acknowledgements

We acknowledge support from the Los Alamos National Laboratory LDRD Program. This work was performed, in part, at the Center for Integrated Nanotechnologies, a US Department of Energy, Office of Basic Energy Sciences Nanoscale Science Research Centre operated jointly by Los Alamos and Sandia National Laboratories. Los Alamos National Laboratory, an affirmative action/equal opportunity employer, is operated by Los Alamos National Security, LLC, for the National Nuclear Security Administration of the US Department of Energy under contract DE-AC52-06NA25396.

References

[1] Zheludev NI. The road ahead for metamaterials. Science 2010;328(5978):582–3.

[2] Soukoulis CM, Wegener M. Optical metamaterials – more bulky and less lossy. Science 2010;330(6011):1633–4.

[3] Boltasseva A, Atwater HA. Low-loss plasmonic metamaterials. Science 2011;331(6015):290–1.

[4] Chen H-T, O'Hara JF, Azad AK, Taylor AJ. Manipulation of terahertz radiation using metamaterials. Laser Photonics Rev 2011;5(4):513–33.

[5] Driscoll T, Palit S, Qazilbash MM, Brehm M, Keilmann F, Chae B-G, Yun S-J, Kim H-T, Cho SY, Jokerst NM, Smith DR, Basov DN. Dynamic tuning of an infrared hybrid-metamaterial resonance using vanadium dioxide. Appl Phys Lett 2008;93(2):024101.

[6] Driscoll T, Kim H-T, Chae B-G, Kim B-J, Lee Y-W, Jokerst NM, Palit S, Smith DR, Di Ventra M, Basov DN. Memory metamaterials. Science 2009;325(5947):1518–21.

[7] Tao H, Strikwerda AC, Fan K, Padilla WJ, Zhang X, Averitt RD. Reconfigurable terahertz metamaterials. Phys Rev Lett 2009;103(14):147401.

[8] Singh R, Azad AK, Jia QX, Taylor AJ, Chen H-T. Thermal tunability in terahertz metamaterials fabricated on strontium titanate single-crystal substrates. Opt Lett 2011;36(7):1230–2.

[9] Chen H-T, Padilla WJ, Zide JMO, Gossard AC, Taylor AJ, Averitt RD. Active terahertz metamaterial devices. Nature 2006;444(7119):597–600.

[10] Shadrivov IV, Morrison SK, Kivshar YS. Tunable split-ring resonators for nonlinear negative-index metamaterials. Opt Express 2006;14(20):9344–9.

[11] Chen H-T, Palit S, Tyler T, Bingham CM, Zide JMO, O'Hara JF, Smith DR, Gossard AC, Averitt RD, Padilla WJ, Jokerst NM, Taylor AJ. Hybrid metamaterials enable fast electrical modulation of freely propagating terahertz waves. Appl Phys Lett 2008;93(9):091117.

[12] Chan WL, Chen H-T, Taylor AJ, Brener I, Cich MJ, Mittleman DM. A spatial light modulator for terahertz beams. Appl Phys Lett 2009;94(21):213511.

[13] Chen H-T, Lu H, Azad AK, Averitt RD, Gossard AC, Trugman SA, O'Hara JF, Taylor AJ. Electronic control of extraordinary terahertz transmission through subwavelength metal hole arrays. Opt Express 2008;16(11):7641–8.

[14] Chen H-T, Padilla WJ, Cich MJ, Azad AK, Averitt RD, Taylor AJ. A metamaterial solid-state terahertz phase modulator. Nat Photon 2009;3(3):148–51.

[15] Padilla WJ, Taylor AJ, Highstrete C, Lee M, Averitt RD. Dynamical electric and magnetic metamaterial response at terahertz frequencies. Phys Rev Lett 2006;96(10):107401.

[16] Chen H-T, Padilla WJ, Zide JMO, Bank SR, Gossard AC, Taylor AJ, Averitt RD. Ultrafast optical switching of terahertz metamaterials fabricated on ErAs/GaAs nanoisland superlattices. Opt Lett 2007;32(12):1620–2.

[17] Degiron A, Mock JJ, Smith DR. Modulating and tuning the response of metamaterials at the unit cell level. Opt Express 2007;15(3):1115–27.

[18] Kim E, Shen YR, Wu W, Ponizovskaya E, Yu Z, Bratkovsky AM, Wang S-Y, Williams RS. Modulation of negative index metamaterials in the near-IR range. Appl Phys Lett 2007;91(17):173105.

[19] Chen H-T, O'Hara JF, Azad AK, Taylor AJ, Averitt RD, Shrekenhamer DB, Padilla WJ. Experimental demonstration of frequency-agile terahertz metamaterials. Nat Photon 2008;2(5):295–8.

[20] Shen N-H, Kafesaki M, Koschny T, Zhang L, Economou EN, Soukoulis CM. Broadband blueshift tunable metamaterials and dual-band switches. Phys Rev B 2009;79(16):161102(R).

[21] Dani KM, Ku Z, Upadhya PC, Prasankumar RP, Brueck SRJ, Taylor AJ. Subpicosecond optical switching with a negative index metamaterial. Nano Lett 2009;9(10):3565–9.
[22] Cho DJ, Wu W, Ponizovskaya E, Chaturvedi P, Bratkovsky AM, Wang S-Y, Zhang X, Wang F, Shen YR. Ultrafast modulation of optical metamaterials. Opt Express 2009;17(20):17652–7.
[23] Shen N-H, Massaouti M, Gokkavas M, Manceau J-M, Ozbay E, Kafesaki M, Koschny T, Tzortzakis S, Soukoulis CM. Optically implemented broadband blueshift switch in the terahertz regime. Phys Rev Lett 2011;106(3):037403.
[24] Dani KM, Ku Z, Upadhya PC, Prasankumar RP, Taylor AJ, Brueck SRJ. Ultrafast nonlinear optical spectroscopy of a dual-band negative index metamaterial all-optical switching device. Opt Express 2011;19(5):3973–83.
[25] Roy Chowdhury D, Singh R, O'Hara JF, Chen H-T, Taylor AJ, Azad AK. Dynamically reconfigurable terahertz metamaterial through photo-doped semiconductor. Appl Phys Lett 2011;99(23):231101.
[26] Singh R, Azad AK, O'Hara JF, Taylor AJ, Zhang W. Effect of metal permittivity on resonant properties of terahertz metamaterials. Opt Lett 2008;33(13):1506–8.
[27] Singh R, Smirnova E, Taylor AJ, O'Hara JF, Zhang W. Optically thin terahertz metamaterials. Opt Express 2008;16(9): 6537–43.
[28] Ricci M, Orloff N, Anlage SM. Superconducting metamaterials. Appl Phys Lett 2005;87(3):034102.
[29] Ricci MC, Anlage SM. Single superconducting split-ring resonator electrodynamics. Appl Phys Lett 2006;88(26):264102.
[30] Ricci MC, Xu H, Prozorov R, Zhuravel AP, Ustinov AV, Anlage SM. Tunability of superconducting metamaterials. IEEE Trans Appl Supercond 2007;17(2):918–21.
[31] Kurter C, Abrahams J, Anlage SM. Miniaturized superconducting metamaterials for radio frequencies. Appl Phys Lett 2010;96(25):253504.
[32] Gu J, Singh R, Tian Z, Cao W, Xing Q, He M, Zhang JW, Han J, Chen H-T, Zhang W. Terahertz superconductor metamaterial. Appl Phys Lett 2010;97(7):071102.
[33] Fedotov VA, Tsiatmas A, Shi JH, Buckingham R, de Groot P, Chen Y, Wang S, Zheludev NI. Temperature control of Fano resonances and transmission in superconducting metamaterials. Opt Express 2010;18(9):9015–9.
[34] Chen H-T, Yang H, Singh R, O'Hara JF, Azad AK, Trugman SA, Jia QX, Taylor AJ. Tuning the resonance in high-temperature superconducting terahertz metamaterials. Phys Rev Lett 2010;105(24):247402.
[35] Jin BB, Zhang C, Engelbrecht S, Pimenov A, Wu J, Xu Q, Cao C, Chen J, Xu W, Kang L, Wu P. Low loss and magnetic field-tunable superconducting terahertz metamaterial. Opt Express 2010;18(16):17504–9.
[36] Kurter C, Zhuravel AP, Ustinov AV, Anlage SM. Microscopic examination of hot spots giving rise to nonlinearity in superconducting resonators. Phys Rev B 2011;84(10):104515.
[37] Kurter C, Tassin P, Zhang L, Koschny T, Zhuravel AP, Ustinov AV, Anlage SM, Soukoulis CM. Classical analogue of electromagnetically induced transparency with a metal-superconductor hybrid metamaterial. Phys Rev Lett 2011;107(4):043901.
[38] Wu J, Jin B, Wan J, Liang L, Zhang Y, Jia T, Cao C, Kang L, Xu W, Chen J, Wu P. Superconducting terahertz metamaterials mimicking electromagnetically induced transparency. Appl Phys Lett 2011;99(16):161113.
[39] Ozyuzer L, Koshelev AE, Kurter C, Gopalsami N, Li Q, Tachiki M, Kadowaki K, Yamamoto T, Minami H, Yamaguchi H, Tachiki T, Gray KE, Kwok W-K, Welp U, Emission of coherent THz radiation from superconductors. Science 2007;318(5854):1291–3.
[40] Du J, Hellicar AD, Li L, Hanham SM, Nicolic N, Macfarlane JC, Leslie KE. Terahertz imaging using a high-Tc superconducting Josephson junction detector. Supercond Sci Technol 2008;21(12):125025.
[41] Chen H-T, O'Hara JF, Taylor AJ, Averitt RD, Highstrete C, Lee M, Padilla WJ. Complementary planar terahertz metamaterials. Opt Express 2007;15(3):1084–95.
[42] Averitt RD, Taylor AJ. Ultrafast optical and far-infrared quasiparticle dynamics in correlated electron materials. J Phys Condens Matter 2002;14(50):R1357–90.
[43] Brorson SD, Buhleier R, Trofimov IE, White JO, Ludwig Ch, Balakirev FF, Habermeier H-U, Kuhl J. Electrodynamics of high-temperature superconductors investigated with coherent terahertz pulse spectroscopy. J Opt Soc Am B 1996;13(9):1979–93.
[44] Terman FE. Radio engineers' handbook. New York: McGraw-Hill; 1943.

Received February 21, 2012; accepted March 24, 2012